American Mineralogist, Volume 95, pages 472–480, 2010

Fantappièite, a new mineral of the cancrinite-sodalite group with a 33-layer stacking sequence: Occurrence and crystal structure

Fernando Cámara,[1] Fabio Bellatreccia,[2,*] Giancarlo Della Ventura,[2] Annibale Mottana,[2] Luca Bindi,[3] Mickey E. Gunter,[4] and Marco Sebastiani[5]

[1]CNR-Istituto di Geoscienze e Georisorse, U.O.S. di Pavia, via Ferrata 1, 27100 Pavia, Italy
[2]Dipartimento Scienze Geologiche, Università Roma Tre, Largo San Leonardo Murialdo 1, 00146 Roma, Italy
[3]Museo di Storia Naturale, Università di Firenze, Sezione di Mineralogia, and CNR-Istituto di Geoscienze e Georisorse, U.O.S. di Firenze, Via La Pira 4, 50121 Firenze, Italy
[4]Department of Geological Sciences, University of Idaho, Moscow, Idaho, 83844-3022, U.S.A.
[5]Dipartimento di Ingegneria Meccanica e Industriale, Università Roma Tre, Via della Vasca Navale 79, I-00146 Roma, Italy

Abstract

This paper reports the occurrence and the crystal structure of fantappièite, a new member of the cancrinite-sodalite group of minerals from Torre Stracciacappe, Trevignano community (Rome, Latium, Italy). The mineral occurs within a volcanic ejectum consisting of dominant sanidine with minor plagioclase, biotite, augitic clinopyroxene, andradite, and iron oxides. Fantappièite (0.7 mm as largest size) is observed within miarolitic cavities of the rock as transparent colorless crystals, showing complex morphologies and striated faces. It is non-pleochroic and uniaxial negative, $n_\omega = 1.5046(5)$ and $n_\varepsilon = 1.5027(5)$. D_{calc} is 2.471 g/cm^3. Fantappièite is trigonal, space group $P\bar{3}$; the cell parameters are: $a = 12.8742(6)$, $c = 87.215(3)$ Å, $V = 12518.8(9)$ Å^3, $Z = 1$. The empirical chemical formula is: $(Na_{84.12}Ca_{30.00}K_{15.95}Fe_{0.19}Ti_{0.13}Mn_{0.10}Mg_{0.09})(Si_{99.36}Al_{98.64})O_{396}(SO_4)_{30.24}(CO_3)_{0.29}Cl_{0.84}F_{0.82}\cdot 5.18H_2O$, which corresponds to the ideal formula $[Na_{82.5}Ca_{33}K_{16.5}]_{\Sigma=132}(Si_{99}Al_{99}O_{396})(SO_4)_{33}\cdot 6H_2O$.

The five strongest reflections in the X-ray powder pattern are [*d* in Å (*I* %) (*hkl*)]: 3.70 (100) (3 0 0), 3.60 (80) (1 0 23), 2.641 (65) (0 0 33), 6.85 (60) (0 1 10), 6.40 (55) (1 1 0).

The single-crystal FTIR spectrum rules out OH groups and shows the presence of H_2O and CO_2 molecules, as well.

The structure can be described as a stacking sequence of 33 layers of six-membered rings of tetrahedra along the *c* axis. The stacking sequence is ACBACABACBACBACBCACBACBACBAB-CBACB…, where A, B, and C represent the positions of the rings within the layers. This sequence gives rise to liottite, sodalite, and cancrinite cages, alternating along *c*. Sulfate groups occur within the liottite cages associated by Na, K, and Ca, while highly disordered sulfate groups are located within the sodalite cages. H_2O groups occur within the cancrinite cages, bonded to Ca and Na cations. Split positions are found for Na-Ca sites, and are related to disordering of the sulfate groups in the sodalite cages.

Keywords: New minerals, fantappièite, crystal structure, IR spectroscopy, mechanical properties

Introduction

The cancrinite group of feldspathoids includes several species structurally characterized by layers of six-membered rings of $[SiO_4]$ and $[AlO_4]$ tetrahedra stacked along the crystallographic *c* direction. The different stacking sequences give rise to different types of structural channels and cages, also extending along the *c*-axis (Bonaccorsi and Merlino 2005). These pores may host several anions and molecular groups, such as H_2O, Cl, CO_3, SO_4, and extra-framework cations such as Na, K, and Ca. The stacking sequence can be simple like …ABABAB (where A and B are the positions in successive layers, using the notation of the closest-packed structures) as in cancrinite sensu stricto, or can be complex, leading to a variety of species for which sequences of 4, 6, 8, 10, 12, 14, 16, 28, and 30 layers for the *c* translation have been described (see Table 2 in Bonaccorsi and Merlino 2005; Chukanov et al. 2008; Rastsvetaeva and Chukanov 2008). Domains with 18 and 24 layer sequences were also observed by transmission electron microscopy (Rinaldi and Wenk 1979). An equal number of layers can also give rise to different sequences, as in marinellite (Bonaccorsi and Orlandi 2003) contrasted with tounkite (Rozenberg et al. 2004), or to different anion-cation populations of the cages. An example of this latter case is represented by afghanite and alloriite that, although having the same type of framework, differ in having Ca-Cl-Ca-Cl (Ballirano et al. 1997) or Na-H_2O-Na-H_2O (Chukanov et al. 2007; Rastsvetaeva et al. 2007) extra-framework contents, respectively. No sequences with an odd number of layers have been found so far. The mineral described here represents the first case of this type of sequence.

* E-mail: bellatre@uniroma3.it

As a matter of fact, Ballirano (1994) on the basis of TEM and FTIR data described an unknown mineral of the cancrinite group from Monte Cavalluccio, Campagnano community (Rome), with a rhombohedral lattice and a cell of a = 12.86 Å and c = 87.3 Å. He proposed a structure made of 33 layers with a prevalence of ABC sequences (corresponding to sodalite). However, due to the lack of a structural model, a formal proposal for a new mineral was never submitted. Recently, a cancrinite-group mineral with a similar c-axis repetition (~87 Å) was found by F.S. Stoppani, a distinguished amateur mineral collector, within the miarolitic cavities of a holocrystalline volcanic ejectum enclosed within a pyroclastic deposit outcrop at Torre Stracciacappe, Trevignano community (Rome), in the Sabatini volcanic complex, Latium (Italy). We succeeded in obtaining a structural model for this mineral, and a formal proposal was submitted to the IMA-CNMNC, which approved the species and the name (IMA 2008-006). The name fantappièite is for Acasto Liberto Fantappiè (Pontassieve, 1862–Viterbo, 1933), a distinguished geologist and naturalist who dedicated part of his scientific activity to the mineralogy and petrology of the volcanic rocks of the Roman Comagmatic Region in the Sabatini area where the mineral has been found. The refined and analyzed crystal is deposited at the Museum of Mineralogy of the University of Roma, La Sapienza (code number MMUR 33027/1).

Occurrence, physical and optical properties

The holocrystalline volcanic ejectum containing fantappièite was found within a pyroclastic deposit consisting of fine-grained ash, enriched with bombs and lithic clasts, cropping out at Torre Stracciacappe, Trevignano community (Rome). The Stracciacappe volcanic center is located in the eastern sector of the Sabatini volcanic complex, which is characterized by mainly explosive volcanic activity beginning about 0.6 Ma. This activity evolved throughout several caldera collapses and the emission of large volumes of pyroclastic and hydromagmatic products (De Rita et al. 1993 and references therein) having the alkaline-potassic signature typical of the Roman Ultrapotassic Province of central Italy. The Stracciacappe crater was active during the last hydromagmatic explosive phase of activity of the Sabatini volcanism between 0.08 and 0.04 Ma (De Rita and Zanetti 1986).

The ejectum, about 10 cm in size, shows a compact outer rim of a greenish fine-grained rock that encloses a dark gray, granular rock rich of small miarolitic cavities. The groundmass of the ejectum consists of interlocking K-feldspar crystals with minor plagioclase, brown mica, and clinopyroxene. Fantappièite occurs within the cavities and it is associated with andradite, augitic clinopyroxene, biotite, and iron oxides. It occurs as transparent colorless crystals, showing complex short-prismatic morphology and frequently striated faces (Fig. 1). The maximum size (probably due to a mosaic of smaller grains) is 0.7 mm in diameter and 0.5 mm along c. The mineral was formed by late-stage metasomatic processes related to the phreatomagmatic stage of the Stracciacappe vent.

Fantappièite has vitreous luster with a white streak and it is not fluorescent; it is brittle with conchoidal fracture; the cleavage is poor on {001} and parting is not observed. The calculated density D_{calc} = 2.471 g/cm^3.

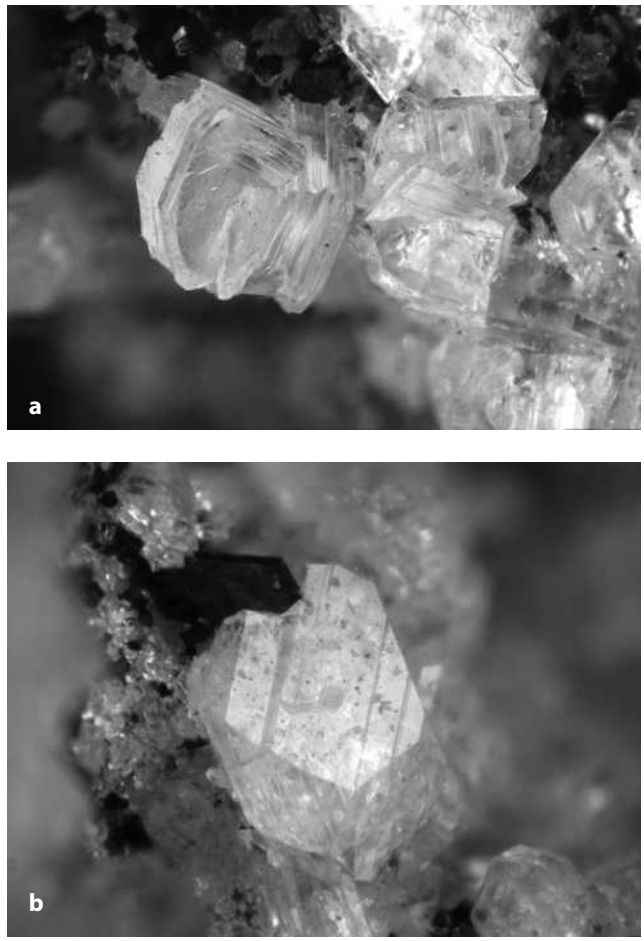

Figure 1. Microphotographs of fantappièite: (**a**) flattened prismatic crystals (0.7 mm), with the typical polysynthetic twinning; (**b**) short-prismatic crystal (0.7 mm in diameter), with striated faces.

Vickers hardness was measured at the Interdepartmental Laboratory of Electron Microscopy (LIME), Università Roma Tre, by means of a Mitutoyo HM-124 microhardness tester, with an applied load of 10 gf (0.1 N) (other test parameters in accordance with ASTM E384 Standard 2008). The average diagonal of the Vickers indent was measured by a Digital Optical Microscope at a magnification of 1000×. Vickers hardness number (VHN) was calculated by the following equation: VHN = 1.8544*(P/d^2), where the applied load P is in kgf, the average dimension d of the indentation marks is in mm, being the resulting hardness number expressed in kgf/mm^2. Results showed an average Vickers hardness of 719.5 kgf/mm^2 (corresponding to about 6 in the Mohs scale) with a standard deviation of 108.0 kgf/mm^2. It is worth noting that the applied load of 10 gf was selected to avoid cracking after indentation, and have a proper evaluation of the actual hardness of the investigated material.

Fantappièite is a non-pleochroic, negative uniaxial mineral with n_ω = 1.5046(5) and n_ε = 1.5027(5). The refractive indices were determined by the double variation method (see Su et al. 1987 and references therein), and the grain was oriented with the spindle stage so as to measure the principal refractive indices (Gunter et al. 2005 and references therein). The compat-

ibility index (Mandarino 1981) is $(1 - K_P)/K_C = -0.0105$ (i.e., superior), indicating excellent agreement between physical and chemical data.

Chemical composition

The microchemical composition of fantappièite was determined using a CAMEBAX 50X WDS-microprobe, at Camparis, Université Paris VI France. Operating conditions were 15 kV accelerating voltage and 4 nA beam current, beam size 20 µm. Counting time was 10 s on both peak and background. Standards, spectral lines, and crystals used were: diopside (Si*K*α, TAP; Ca*K*α, PET, Mg*K*α, TAP), orthoclase (Al*K*α, TAP, K*K*α, PET), albite (Na*K*α, TAP), Fe_2O_3 (Fe*K*α, LIF), titanite (Ti*K*α, LIF), $MnTiO_3$ (Mn*K*α, LIF), pyrite (S*K*α, PET), vanadinite (Cl*K*α, PET), and fluorite (F*K*α, TAP). Analytical errors are 1% rel. for major elements and 5% rel. for minor elements. Data reduction was done using the PAP method (Pouchou and Pichoir 1985). The analysis and empirical chemical formula, based on 198 Si+Al atoms, are given in Table 1; site populations are based on the structure refinement. The simplified, ideal, charge-balanced formula is: $[Na_{82.5}Ca_{33}K_{16.5}]_{\Sigma=132}(Si_{99}Al_{99}O_{396})(SO_4)_{33}\cdot 6H_2O$, simplified as $\{[Na_5Ca_2K]_{\Sigma=8}(Si_6Al_6O_{24})(SO_4)_2\cdot 0.36H_2O\}\cdot 16.5$, which requires: K_2O 4.106, Na_2O 13.506, CaO 9.776, Al_2O_3 26.662, SiO_2 31.421, SO_3 13.957, H_2O 0.571, Total 100.00 wt%. The H_2O content was calculated and checked by the structural model, assuming that the H_2O groups are hosted only in the six cancrinite cages; FTIR spectroscopy (see below) showed only H_2O, and no OH, in the studied sample. FTIR spectroscopy also shows the presence of some CO_2; its content was then calculated (Table 1) on the basis of the chemical analysis from charge-balance requirements, following the method described in Ballirano et al. (1996).

X-ray diffraction and description of the structure

The powder pattern of fantappièite was collected at the Centro Interdipartimentale di Cristallografia Strutturale (CRIST), Università di Firenze (Table 2), with a 114.6 mm Gandolfi camera (Ni-filtered Cu*K*α; exposure time 96 h). Peak intensities were measured with an automated densitometer and the pattern was indexed on the basis of the powder spectra calculated from the crystal structure (see below). The cell parameters, refined with the least squares program Unitcell (Holland and Redfern 1997), are: $a = 12.8095(5)$, $c = 87.298(4)$ Å, $V = 12405.1(9)$ Å^3.

Table 1. EMP analysis and empirical formula of fantappièite calculated on the basis of Σ(Si+Al) = 198 apfu

	wt%	Range		apfu
SiO_2	32.193	32.02–32.50	Si	99.36
Al_2O_3	27.117	26.60–27.60	Al	98.64
FeO	0.073	0.00–0.18	Σ	198.00
K_2O	4.050	3.80–4.31		
CaO	9.073	8.88–9.19	Ca	30.00
Na_2O	14.058	13.78–14.51	Fe^{2+}	0.19
MgO	0.020	0.00–0.04	K	15.95
MnO	0.038	0.00–0.12	Na	84.12
TiO_2	0.056	0.00–0.16	Ti	0.13
SO_3	13.056	12.23–13.49	Mg	0.09
Cl	0.161	0.14–0.21	Mn	0.10
F	0.084	0.00–0.39	Σ	130.58
H_2O†	0.503			
CO_2*	0.069		SO_4^{2-}	30.24
	100.552		Cl^-	0.84
–O=F,Cl	0.072		F^-	0.82
Total	100.480		H_2O†	5.18
			CO_3^{2-}*	0.29

* Calcutated according to Ballirano et al. (1996).
† Calculated assuming Σ(H_2O+F) = 6 apfu (see text).

Structure determination and refinement

A crystal of 20 × 20 × 35 µm was used for single-crystal X-ray diffraction using a Oxford Diffraction Excalibur PX Ultra, under Cu*K*α (λ = 1.54138 Å) radiation and working at 50 kV and 40 mA, at the CRIST. Data were collected at 100 K using an Oxford cryostream cooler. Crystal-to-detector distance was 7 cm. A total of 3440 frames was collected, consisting of 5 sets of omega runs with an exposure time of 200 s per frame and a frame width of 0.45°. Data were processed using the CrysAlis software package version 1.171.31.2 (Oxford Diffraction 2006) running on the Xcalibur PX control PC. A relatively high sin(θ)/λ cutoff and a high redundancy were chosen in the recording settings. Intensity integration and standard Lorentz-polarization correction were performed with the CrysAlis RED (Oxford Diffraction Ltd.) software package version 1.171.31.2. The program ABSPACK in CrysAlis RED was applied for the absorption correction. Unit-cell dimensions (Table 3) were calculated from

Table 2. Powder diffraction data for fantappièite

hkl	d_{obs} (Å)	d_{calc} (Å)	$2\theta_{obs}$ (°)	$2\theta_{calc}$ (°)	Δ2θ (°)	I/I_0 (%)
0 1 10	6.850	6.860	12.913	12.895	0.019	60
1 1 0	6.400	6.402	13.826	13.822	0.004	55
2 $\bar{1}$ 3; 1 1 3	6.250	6.252	14.159	14.154	0.005	5
0 1 13	5.740	5.745	15.424	15.412	0.013	45
0 2 2	5.490	5.500	16.131	16.102	0.029	10
3 $\bar{1}$ 2; 2 1 2	4.180	4.186	21.238	21.208	0.031	10
1 0 20	4.060	4.062	21.874	21.862	0.012	10
1 2 10; $\bar{1}$ 3 10; 02 17	3.780	3.778	23.516	23.528	–0.011	55
3 0 0; 0 3 3; 2 1 11; 3 $\bar{1}$ 11	3.700	3.696	24.032	24.059	–0.026	100
1 0 23	3.600	3.592	24.710	24.769	–0.059	80
1 2 13; $\bar{1}$ 3 13	3.560	3.556	24.992	25.025	–0.032	50
2 1 14; 2 $\bar{1}$ 21; 3 $\bar{1}$ 14; 1 1 21	3.480	3.478	25.577	25.588	–0.011	10
0 1 25; $\bar{1}$ 3 16; 1 2 16	3.320	3.324	26.832	26.800	0.031	25
3 $\bar{1}$ 17; 2 1 17	3.240	3.247	27.507	27.446	0.061	20
1 2 19; $\bar{1}$ 3 19	3.090	3.097	28.871	28.808	0.063	5
2 1 20; 3 $\bar{1}$ 20	3.020	3.023	29.555	29.522	0.033	25
3 1 10; 4 $\bar{1}$ 10; 0 0 30	2.895	2.901	30.862	30.801	0.061	15
1 3 11	2.868	2.868	31.160	31.165	–0.005	10
0 3 21; 4 0 5	2.762	2.762	32.388	32.383	0.005	10
4 0 8; 4 $\bar{1}$ 16; 3 1 16	2.685	2.687	33.344	33.322	0.022	10
0 4 10; 0 0 33; 4 0 11; 1 3 17; $\bar{1}$ 4 17	2.641	2.642	33.916	33.902	0.014	65
0 3 24	2.593	2.593	34.563	34.566	–0.003	5
0 4 13	2.561	2.562	35.009	34.990	0.019	10
4 0 14	2.539	2.543	35.322	35.269	0.053	10
4 0 17; 1 1 33	2.442	2.445	36.774	36.723	0.051	15
0 0 36	2.421	2.420	37.105	37.127	–0.022	10
$\bar{1}$ 4 23; 1 3 23	2.390	2.390	37.604	37.611	–0.007	5
4 0 20	2.340	2.340	38.439	38.437	0.002	10
4 0 23	2.240	2.239	40.227	40.251	–0.024	35
0 3 33; 3 0 33	2.150	2.151	41.989	41.960	0.029	25
3 3 0	2.134	2.134	42.319	42.321	–0.003	35
4 0 29	2.039	2.039	44.393	44.385	0.008	5
0 3 36; 3 0 36	2.028	2.028	44.646	44.651	–0.005	5
0 1 46	1.872	1.871	48.596	48.625	–0.029	10
1 2 43; $\bar{1}$ 3 43	1.829	1.827	49.815	49.863	–0.047	5
1 4 33; $\bar{1}$ 5 33; 4 1 33; 5 $\bar{1}$ 33	1.786	1.786	51.100	51.113	–0.013	15
5 2 0; 2 5 0	1.779	1.775	51.315	51.424	–0.109	5
0 4 43	1.640	1.640	56.029	56.039	–0.010	10

Notes: Ni-filtered Cu*K*α; exposition: 96 h; 114.6 mm Gandolfi camera. Indices calculated from structural model with XPow software (Downs et al. 1993). Only the indices of the reflections with calculated intensity >0.5 are given.

least-squares refinement of the position of 321 reflections in the 8–15.7 °θ range.

Most intense reflections were compatible with a rhombohedral lattice and 3*m*1 Laue symmetry. However, there were evident violations to the *R*-centering not compatible with obverse-reverse twinning in a rhombohedral lattice. The structure was then solved in the space group $P\bar{3}$ by direct methods using SIR 2004 (Burla et al. 2005), which supplied an incomplete model consisting mainly of framework cations and anions. The resulting structure had an ACBACABACBACBACBCACBACBACBABCBACB… stacking sequence, where A, B, and C represent the positions of the rings within the layers. Following the Zhdanov notation (Zhdanov 1945; Patterson and Kasper 1959), the observed basic partition is (9)(2)(9)(2)(9)(2) and the sequence can be expressed just as 3 × 11 [(9)(2)]. Based on these results, the structure should have a rhombohedral lattice with space group $R\bar{3}m$. EMP analysis provides a Si/Al = 1, thus, in accordance with the Löwenstein rule (Löwenstein 1954) and with all the previous structure refinements done on minerals of the cancrinite-sodalite group, a long-range ordering of Si and Al in the tetrahedral sites is expected (Bonaccorsi and Merlino 2005). The presence of mirror planes would avoid the usual ordering of Al and Si tetrahedra in the framework and therefore the symmetry has to be reduced to $R\bar{3}$. Accordingly, we have found different crystals with differing degrees of *R* lattice violations, although reflections violating the *R* lattice are always weak, and their intensity varies from crystal to crystal. The observed reduction of symmetry to $P\bar{3}$ must be ascribed to the ordering of extra-framework cations and anions. Hence the structure was refined in space group $P\bar{3}$; a total of 4594 unique reflections with $R_{int} = 0.075$ were used for full-matrix weighted least-squares refinement on F_o^2; alternating difference Fourier maps and refinement cycles were performed to approach convergence using SHELX-97 (Sheldrick 2008). However, the observed agreement factor was high, leading to the suspicion of merohedral twinning, as it is found frequently in minerals of the cancrinite group with complex stacking sequences. The PLATON/TwinRotMat (Spek 2008) indicated the possible presence of up to three twin operations: twofold rotation about (100) with twin matrix (110/0$\bar{1}$0/00$\bar{1}$); twofold rotation about (001) with twin matrix ($\bar{1}$00/0$\bar{1}$0/001); and twofold rotation about (110) with twin matrix (010/100/00$\bar{1}$). The same program routine was used to produce an HKLF5 file for twin refinement with SHELX-97. The twin fractions refined to 0.17(1), 0.018(4), and 0.36(4), respectively. Scattering factors were taken from the *International Tables for X-ray Crystallography* (Wilson 1992). Neutral scattering curves were used for all elements. Anisotropic displacement factors were calculated for all atom positions except the Na atoms and the O atoms coordinating S in the SO_4 groups and those representing H_2O groups. Some of the SO_4 groups present high disorder and it was not possible to locate the position of the coordinating O atoms. At convergence, a model with 175 atoms resulted in agreement factors of $R = 0.0610$ for 4171 reflections with $I > 2\sigma(I)$, and $R = 0.0652$ for all 4594 unique reflections, and a goodness of fit factor of 1.073. Table 3 reports the results of the refinement. Table 4 reports selected bond distances. Final coordinates and displacement parameters are reported in Table 5[1]. Table 6[1] lists the anisotropic displacement parameters and Table 7[1] lists the observed and calculated structure factors.

TABLE 3. Crystal data and structure refinement for fantappièite

Crystal system, space group	trigonal, $P\bar{3}$
Unit-cell dimensions (Å)	$a = 12.8742(6)$
	$b = 12.8742(6)$
	$c = 87.215(3)$
Volume (Å^3)	12518.8(9)
Z	1
Temperature (K)	100(2)
Wavelength (Å)	1.54184
Crystal size (mm)	0.04 × 0.02 × 0.02
Absorption coefficient (mm^{-1})	10.527
θ range for data collection (°)	5.00 to 39.99
Limiting indices	$-10 \le h \le 10$
	$-10 \le k \le 10$
	$-64 \le l \le 64$
F(000)	8471
Reflections collected/unique	23430/4594 [$R_{int} = 0.0751$]
Completeness to theta = 39.99°	89.6%
Max. and min. transmission	0.903 and 0.790
Refinement method	Full-matrix least-squares on F^2
Data/restraints/parameters	4594/721/1194
Goodness-of-fit on F^2	1.073
Final R indices [$I > 2\sigma(I)$]	$R = 0.0610$, w$R^2 = 0.1607$
R indices (all data)	$R = 0.0652$, w$R^2 = 0.1645$
Largest diff. peak and hole (e$^-$/Å^3)	+0.835/–0.804

FTIR SPECTROSCOPY

The powder FTIR spectrum of fantappièite was collected on a Nicolet Magna 760 FTIR spectrometer equipped with a DTGS detector and a KBr beamsplitter; the nominal resolution was 4 cm^{-1} and 64 scans were averaged for each sample and for the background. The spectra were collected on a KBr disk with about 1 mg of sample in 150 mg of KBr. Single-crystal FTIR spectra were collected on crystal fragments ~30 μm thick using a NicPlan microscope equipped with a liquid nitrogen-cooled MCT detector; the nominal resolution was 4 cm^{-1} and 128 scans were averaged for each sample and for the background.

The powder infrared spectrum of fantappièite (Fig. 2) is different than the spectra of other cancrinite-group minerals, but shows close similarities with the spectrum of franzinite given by Ballirano et al. (1996, 2000). A weak absorption assigned to the bending mode (ν_2) of the H_2O molecule(s) is found around 1634 cm^{-1} (Fig. 2a); a very intense, multi-component absorption is observed in the 1200–1000 cm^{-1} region, which can be assigned to the vibrations of the SO_4^{2-} groups (peaks at 1153 and 1113 cm^{-1}) and to framework (Si,Al)-O stretching (peaks at 1037 and 1006 cm^{-1}) (Moenke 1974; Ross 1974).

In the 800–400 cm^{-1} region (Fig. 2b), there is a group of well-defined bands at 790, 699, 645, and 614 cm^{-1} plus two evident shoulders at 730 and 592 cm^{-1}. Finally, a very intense and convoluted absorption is observed at around 447 cm^{-1}. Figure 2b displays an enlargement of the spectrum of fantappièite in comparison with that of franzinite where the similarity of the two patterns is apparent. There are however some fine details (starred in Fig. 2b), which can be used to distinguish the two species from one another, and from the other cancrinite-group minerals.

[1] Deposit item AM-10-017, Tables 5, 6, and 7 and a data set. Deposit items are available two ways: For a paper copy contact the Business Office of the Mineralogical Society of America (see inside front cover of recent issue) for price information. For an electronic copy visit the MSA web site at http://www.minsocam.org, go to the *American Mineralogist* Contents, find the table of contents for the specific volume/issue wanted, and then click on the deposit link there.

The unpolarized-light single-crystal FTIR spectrum in the 4000–1500 cm^{-1} range (Fig. 3), shows an intense absorption at 1634 cm^{-1} that is assigned to the ν_2 water bending mode; a second band on the higher frequency side of the first component, centered at 1693 cm^{-1} is also present, whose assignment is still uncertain.

The broad band centered around 2100 cm^{-1} can be related to the first overtone of the stretching modes of the (Si,Al)-O and SO_4^{2-} absorptions (Della Ventura et al. 2008). The very sharp peak at 2388 cm^{-1} indicates the presence of CO_2 molecules in the structural pores of fantappièite (Della Ventura et al. 2005).

A broad absorption extending from about 2500 to 3700 cm^{-1} can be resolved into three main components at 3241, 3580, and 3622 cm^{-1} plus a pronounced shoulder at 3406 cm^{-1}. These absorptions can be attributed to the stretching (ν_1 and ν_3) and the first overtone of the bending modes ($2\nu_2$) of H_2O. Finally, a band at 5243 cm^{-1} is assigned to the combination of the stretching (ν_3) + bending (ν_2) modes of H_2O (Ihinger et al. 1994). The absence of bands in the 4300–4100 cm^{-1} range, due to the combination modes of the OH group (Ihinger et al. 1994), rules out the presence of hydroxyl groups in fantappièite.

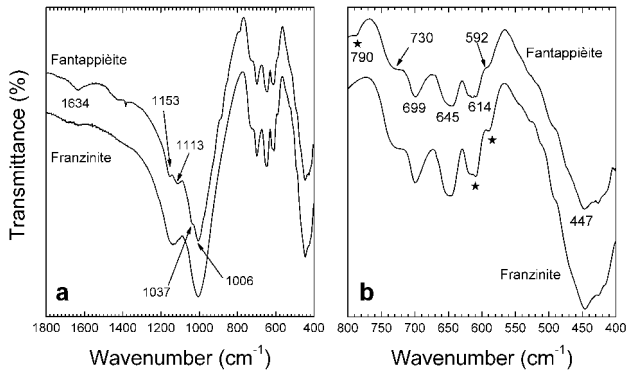

FIGURE 2. FTIR powder spectrum of fantappièite compared to the spectrum of franzinite: (**a**) the region of H_2O (bending), SO_4^{2-} and $(Si,Al)O_4$ absorptions; (**b**) detail of the <800 cm^{-1} region. The stars indicate the very subtle details that differentiate the spectra of fantappièite and franzinite.

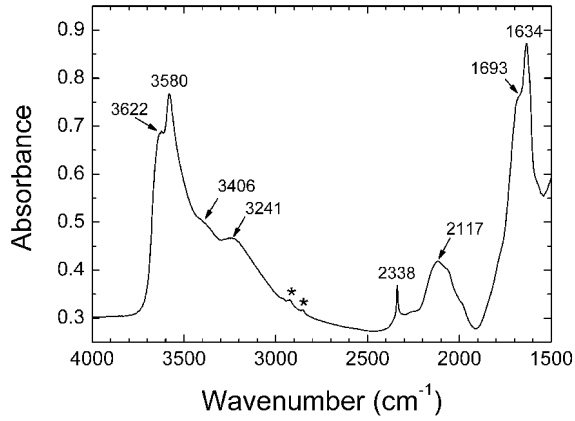

FIGURE 3. Unpolarized light single-crystal FTIR spectrum of fantappièite. (* = grease.)

DESCRIPTION OF THE CRYSTAL STRUCTURE

The observed stacking sequence for the framework of fantappièite is ACBACABACBACBACBCACBACBACBABCBACB. The structure has 6 bystrite (losod) cages (B), 21

TABLE 4a. Selected bond distances (Å) of the framework polyehedra for fantappièite

T1-O2	1.517 (12)	T10-O39	1.552 (11)	T19-O12	1.591 (10)
T1-O1_$12	1.60 (2)	T10-O40_$4	1.648 (11)	T19-O8_$4	1.614 (12)
T1-O3_$2	1.651 (11)	T10-O38	1.648 (12)	T19-O10_$7	1.623 (12)
T1-O5	1.720 (11)	T10-O36	1.675 (10)	T19-O11	1.656 (10)
<T1-O>	1.623	<T10-O>	1.631	<T19-O>	1.621
T2-O7	1.595 (9)	T11-O43_$2	1.62 (2)	T20-O15_$2	1.611 (13)
T2-O4	1.663 (13)	T11-O42	1.681 (13)	T20-O16	1.685 (14)
T2-O6_$5	1.670 (10)	T11-O45	1.698 (12)	T20-O13	1.71 (1)
T2-O8	1.701 (12)	T11-O41	1.76 (2)	T20-O14	1.717 (12)
<T2-O>	1.657	<T11-O>	1.690	<T20-O>	1.680
T3-O9	1.584 (10)	T12-O47_$4	1.624 (11)	T21-O17_$5	1.619 (13)
T3-O11	1.646 (11)	T12-O44_$4	1.66 (2)	T21-O19	1.641 (12)
T3-O13	1.672 (14)	T12-O49	1.671 (12)	T21-O21	1.692 (9)
T3-O10	1.739 (12)	T12-O46	1.795 (14)	T21-O18_$5	1.743 (9)
<T3-O>	1.660	<T12-O>	1.687	<T21-O>	1.674
T4-O14	1.535 (11)	T13-O51	1.563 (13)	T22-O22	1.696 (9)
T4-O17_$5	1.762 (13)	T13-O48	1.59 (1)	T22-O23	1.702 (8)
T4-O15	1.783 (13)	T13-O53_$2	1.666 (12)	T22-O25	1.753 (8)
T4-O12_$5	1.804 (11)	T13-O50_$6	1.745 (12)	T22-O20	1.755 (8)
<T4-O>	1.721	<T13-O>	1.640	<T22-O>	1.726
T5-O20	1.567 (10)	T14-O52_$5	1.637 (10)	T23-O26	1.575 (11)
T5-O18	1.717 (10)	T14-O56	1.659 (12)	T23-O29_$2	1.618 (13)
T5-O16	1.723 (14)	T14-O55	1.693 (11)	T23-O24_$6	1.710 (12)
T5-O19	1.775 (10)	T14-O54	1.731 (14)	T23-O27_$6	1.77 (2)
<T5-O>	1.695	<T14-O>	1.680	<T23-O>	1.668
T6-O21	1.581 (10)	T15-O58	1.598 (12)	T24-O28	1.627 (11)
T6-O22_$1	1.632 (11)	T15-O61	1.632 (13)	T24-O30	1.686 (13)
T6-O24_$5	1.670 (12)	T15-O57_$2	1.720 (11)	T24-O33	1.688 (10)
T6-O23	1.733 (10)	T15-O60	1.782 (12)	T24-O31	1.720 (13)
<T6-O>	1.654	<T15-O>	1.683	<T24-O>	1.68
T7-O27	1.60 (2)	T16-O59_$4	1.621 (11)	T25-O35_$4	1.586 (10)
T7-O25	1.619 (11)	T16-O66_$11	1.671 (11)	T25-O34	1.711 (8)
T7-O28	1.678 (11)	T16-O62	1.689 (14)	T25-O32_$4	1.720 (13)
T7-O26	1.774 (11)	T16-O63_$7	1.725 (12)	T25-O36	1.790 (9)
<T7-O>	1.667	<T16-O>	1.677	<T25-O>	1.70
T8-O29	1.533 (13)	T17-O3	1.600 (11)	T26-O41	1.54 (2)
T8-O32	1.603 (12)	T17-O2	1.664 (12)	T26-O37	1.589 (11)
T8-O30	1.624 (13)	T17-O4	1.712 (13)	T26-O39	1.653 (11)
T8-O31_$1	1.729 (13)	T17-O1_$5	1.73 (2)	T26-O38_$6	1.693 (12)
<T8-O>	1.622	<T17-O>	1.675	<T26-O>	1.617
T9-O34	1.604 (7)	T18-O6	1.602 (8)	T27-O44	1.56 (2)
T9-O33	1.678 (8)	T18-O5	1.630 (9)	T27-O42	1.637 (13)
T9-O35	1.703 (8)	T18-O9	1.663 (8)	T27-O40	1.680 (12)
T9-O37	1.738 (9)	T18-O7	1.680 (8)	T27-O43	1.69 (2)
<T9-O>	1.681	<T18-O>	1.644	<T27-O>	1.641
T28-O46	1.598 (14)	T30-O53	1.539 (9)	T32-O63	1.630 (12)
T28-O45	1.606 (12)	T30-O57	1.578 (9)	T32-O61	1.635 (13)
T28-O48	1.67 (1)	T30-O54_$1	1.623 (14)	T32-O62	1.701 (14)
T28-O47	1.684 (11)	T30-O55	1.686 (13)	T32-O64	1.770 (12)
<T28-O>	1.640	<T30-O>	1.606	<T32-O>	1.684
T29-O49	1.525 (12)	T31-O60	1.567 (12)	T33-O64	1.605 (12)
T29-O50	1.586 (12)	T31-O56	1.614 (12)	T33-O65_$11	1.654 (11)
T29-O52	1.662 (11)	T31-O59	1.746 (10)	T33-O65	1.663 (11)
T29-O51	1.720 (14)	T31-O58_$5	1.794 (11)	T33-O66	1.694 (12)
<T29-O>	1.623	<T31-O>	1.680	<T33-O>	1.654

Notes: Symmetry operators $1: *–y*+1, *x–y*, *z*; $2: *–x*+*y*+1, *–x*+1, *z*; $3: *x–y*, *x*, *–z*; $4: *–y*, *x–y*, *z*; $5: *–x*+*y*, *–x*, *z*; $6: *-y*+1, *x–y*+1, *z*; $7: *–x*+*y*, *–x*+1, *z*; $8: *y*, *–x*+*y*, *–z*+1; $9: *–x*+1, *–y*+1, *–z*+1; $10: *–x*, *–y*, *–z*+1; $11: *x–y*, *x*, *–z*+1; $12: *y*, *–x*+*y*, *–z*; $13: *x*, *y*+1, *z*; $14: *x*, *y*–1, *z*; $15: *–x*, *–y*, *–z*.

TABLE 4B. Selected distances for extra-framework polyhedra

Ca1-O5SA	2.263(12)	Ca9-O55_$2	2.48(2)	Na1B-O1_$12	2.84(2)	Na9B-Na9A	0.88(5)	Na20-Ca8	1.97(2)
Ca1-O11_$7	2.610(12)	Ca9-O54_$1	2.657(12)	<Na1B-O>	2.68	Na9B-O31	2.301(15)	Na20-O3W	2.34(3)
Ca1-O11_$6	2.610(12)	Ca9-O54	2.657(12)	Na2-O2	2.537(13)	Na9B-O36_$6	2.518(13)	Na20-O51	2.88(1)
Ca1-O11	2.610(12)	Ca9-O54_$2	2.657(12)	Na2-O3	2.557(10)	Na9B-O33	2.557(14)	<Na20-O>	2.61
Ca1-O10_$6	2.687(10)	<Ca9-O>	2.506	<Na2-O>	2.547	Na9B-O37	2.66(2)	Na21-O47	2.510(13)
Ca1-O10_$7	2.687(10)	Ca10-O13B	2.221(9)	Na3A-Na3B	1.61(3)	Na9B-O32_$2	2.669(14)	Na21-O54	2.63(1)
Ca1-O10	2.687(10)	Ca10-O59	2.346(11)	Na3A-O7	2.525(9)	Na9B-O38_$6	2.995(14)	Na21-O48	2.67(2)
<Ca1-O>	2.594	Ca10-O12B_$5	2.40(2)	Na3A-O6	2.785(11)	<Na9B-O>	2.616	Na21-O49_$5	2.680(14)
Ca2-O5SB	2.269(9)	Ca10-O57	2.446(11)	<Na3A-O>	2.655	Na10-Na11	1.84(3)	Na21-O53_$2	2.691(14)
Ca2-O13	2.410(14)	Ca10-O61_$1	2.488(13)	Na3B-Na3A	1.61(3)	Na10-O38	2.390(13)	Na21-O52_$5	2.697(13)
Ca2-O16	2.414(14)	Ca10-O63_$1	2.530(13)	Na3B-O7	2.594(14	<Na10-O>	2.390	<Na21-O>	2.646
Ca2-O12	2.547(12)	Ca10-O56	2.692(13)	Na3B-O6	3.02(2)	Na11-Na10	1.84(3)	Na22-Na23	1.00(2)
Ca2-O17	2.657(13)	Ca10-O55	2.93(2)	<Na3B-O>	2.805	Na11-O38	2.512(12)	Na22-O52	2.376(13)
Ca2-O18	2.714(14)	<Ca10-O>	2.508	Na4A-Na4B	0.89(2)	Na11-O39	2.868(10)	Na22-O53_$2	2.412(14)
Ca2-O11	2.928(14)	Ca11-O14A_$9	2.23(11)	Na4A-O4	2.46(2)	<Na11-O>	2.690	Na22-O58	2.56(2)
<Ca2-O>	2.563	Ca11-O62_$7	2.54(13)	Na4A-O3	2.54(1)	Na12-Na13	0.81(2)	Na22-O51	2.69(2)
Ca3-O7SA	2.099(11)	Ca11-O62_$6	2.54(13)	Na4A-O10_$1	2.55(2)	Na12-O40	2.57(2)	Na22-O56_$4	2.80(1)
Ca3-O19_$5	2.292(11)	Ca11-O62	2.54(13)	Na4A-O5_$1	2.60(2)	Na12-O41	2.57(2)	Na22-O57_$2	2.938(14)
Ca3-O19	2.292(11)	Ca11-O12B	2.76(2)	Na4A-O9_$1	2.69(1)	Na12-O35	2.62(2)	<Na22-O>	2.63
Ca3-O19_$4	2.292(11)	Ca11-O12B_$7	2.76(2)	Na4A-O8	2.75(2)	Na12-O37	2.68(2)	Na23-Na22	1.00(2)
Ca3-O18	2.715(11)	Ca11-O12B_$6	2.76(2)	<Na4A-O>	2.598	Na12-O36_$5	2.81(2)	Na23-O58	2.44(2)
Ca3-O18_$4	2.715(11)	<Ca11-O>	2.590	Na4B-Na4A	0.89(2)	Na12-O42	3.00(2)	Na23-O53_$2	2.68(2)
Ca3-O18_$5	2.715(11)	K1-O17_$6	2.753(13)	Na4B-O8	2.57(2)	<Na12-O>	2.71	Na23-O57_$2	2.71(2)
<Ca3-O>	2.446	K1-O16	2.777(14)	Na4B-O10_$1	2.58(2)	Na13-Na12	0.81(2)	Na23-O56_$4	2.81(2)
Ca4-O6SB	2.331(8)	K1-O5SB	2.810(11)	Na4B-O9_$1	2.61(2)	Na13-O40	2.29(2)	Na23-O52	2.83(2)
Ca4-O24	2.424(11)	K1-O6SB_$6	2.813(11)	Na4B-O3	2.74(2)	Na13-O41	2.52(2)	Na23-O51	2.96(2)
Ca4-O25	2.458(12)	K1-O20	2.846(12)	Na4B-O4	2.74(2)	Na13-O35	2.54(2)	<Na23-O>	2.74
Ca4-O7SB	2.529(12)	K1-O21_$2	2.906(11)	Na4B-O5_$1	2.92(2)	Na13-O36_$5	2.80(2)	Na24-O60	2.492(12)
Ca4-O20	2.570(12)	K1-O5SB_$6	2.911(11)	<Na4B-O>	2.695	Na13-O37	2.83(2)	Na24-O58	2.846(12)
Ca4-O21_$4	2.626(11)	K1-O6SB	2.967(11)	Na5A-Na5B	1.02(2)	Na13-O42	3.00(2)	<Na24-O>	2.669
<Ca4-O>	2.490	K1-O22	3.043(12)	Na5A-O8	2.34(2)	<Na13-O>	2.66	Na25-O66_$9	2.360(10)
Ca5-O6SA	2.116(13)	<K1-O>	2.870	Na5A-O9	2.37(2)	Na14-Na15	1.69(3)	Na25-O66	2.360(10)
Ca5-O26_$6	2.438(9)	K2-O8SB	2.702(12)	Na5A-O14	2.64(2)	Na14-O42	2.48(2)	Na25-O64	2.425(11)
Ca5-O26_$7	2.438(9)	K2-O28	2.734(10)	Na5A-O12_$5	2.80(2)	Na14-Cl1	3.28(3)	Na25-O64_$9	2.425(11)
Ca5-O26	2.438(9)	K2-O7SB	2.770(16)	Na5A-O13	2.85(2)	<Na14-O>	2.68	Na25-O14B_$2	2.475(8)
Ca5-O27_$7	2.994(14)	K2-O7SB_$5	2.800(17)	Na5A-O7	2.90(2)	Na15-Na14	1.69(3)	Na25-O14B_$11	2.475(8)
Ca5-O27_$6	2.994(14)	K2-O25	2.833(12)	<Na5A-O>	2.651	Na15-O42	2.342(12)	Na25-O63_$9	2.998(11)
Ca5-O27	2.994(14)	K2-O8SB_$5	2.859(13)	Na5B-Na5A	1.02(2)	Na15-O43	2.771(13)	Na25-O63	2.998(11)
<Ca5-O>	2.630	K2-O29	2.926(13)	Na5B-O9	2.573(13)	<Na15-O>	2.556	<Na25-O>	2.564
Ca6-O8SB	2.295(11)	K2-O24_$5	2.959(11)	Na5B-O8	2.589(14)	Na16-Na17	0.814(12)	Na26-O65	2.720(9)
Ca6-O27	2.51(2)	K2-O23	3.291(12)	Na5B-O14	2.602(13)	Na16-O46	2.424(16)	<Na26-O>	2.720
Ca6-O33	2.523(12)	<K2-O>	2.875	Na5B-O12_$5	2.626(13)	Na16-O39	2.734(13)		
Ca6-O32_$4	2.618(13)	K3-O14B_$2	2.765(11)	Na5B-O13	2.64(2)	Na16-O40_$4	2.738(12)	S5-O5SA	1.507(5)
Ca6-O28	2.647(11)	K3-O14B	2.813(11)	Na5B-O7	2.917(13)	Na16-O41	2.824(17)	S5-O5SB	1.510(5)
Ca6-O29_$4	2.744(13)	K3-O13B	2.817(11)	<Na5B-O>	2.658	Na16-O44_$4	2.888(16)	<S5-O>	1.509
Ca6-O34	2.965(12)	K3-O59	2.850(11)	Na6-O15	2.419(14)	<Na16-O45	2.941(13)	S6-O6SA	1.508(5)
<Ca6-O>	2.615	K3-O13B_$2	2.866(11)	Na6-O14	2.685(10)	Na16-O>	2.758	S6-O6SB	1.499(5)
Ca7-O8SA	2.073(13)	K3-O61	2.906(13)	<Na6-O>	2.552	Na17-Na16	0.814(12)	<S6-O>	1.501
Ca7-O34	2.586(10)	K3-O64	2.988(11)	Na7-O23	2.611(11)	Na17-O39	2.337(16)	S7-O7SA	1.516(5)
Ca7-O34_$5	2.586(10)	K3-O66_$8	3.040(10)	Na7-O22	2.622(11)	Na17-O41	2.643(20)	S7-O7SB	1.514(5)
Ca7-O34_$4	2.586(10)	K3-O65	3.251(11)	Na7-O1W	2.63(4)	Na17-O40_$4	2.673(15)	<S7-O>	1.515
Ca7-O35_$5	2.720(9)	<K3-O>	2.922	<Na7-O>	2.618	Na17-O46	2.706(19)	S8-O8SA	1.516(5)
Ca7-O35	2.720(9)	Na1A-Na1B	1.049(14)	Na8-O30	2.466(13)	Na17-O45	2.866(16)	S8-O8SB	1.516(5)
Ca7-O35_$4	2.720(9)	Na1A-O1	2.49(2)	Na8-O31	2.872(11)	Na17-O44_$4	2.905(19)	<S8-O>	1.516
<Ca7-O>	2.570	Na1A-O1_$12	2.53(2)	Na8-Cl1	2.97(2)	<Na17-O>	2.688	S12-S12_$6	0.55(3)
Ca8-Na20	1.97(2)	Na1A-O5	2.61(2)	<Na8-O>	2.712	Na18-O46	2.520(12)	S12-O12B_$7	1.464(2)
Ca8-O51_$7	2.579(11)	Na1A-O6	2.67(2)	Na9A-Na9B	0.88(5)	Na18-O47	2.586(9)	S12-O12B_$6	1.762(4)
Ca8-O51	2.579(12)	Na1A-O2_$3	2.76(2)	Na9A-O31	2.65(5)	<Na18-O>	2.553	S12-O12B	1.976(2)
Ca8-O51_$6	2.579(12)	Na1A-O4_$4	2.80(2)	Na9A-O33	2.66(4)	Na19-O50_$5	2.336(13)		
Ca8-O50	3.089(10)	<Na1A-O>	2.64	Na9A-O36_$6	2.81(5)	Na19-O43	2.57(2)	S13-O13A	1.516(5)
Ca8-O50_$7	3.089(10)	Na1B-Na1A	1.049(14)	Na9A-O2W	2.81(5)	Na19-O49_$5	2.579(13)	S13-O13B	1.507(5)
Ca8-O50_$6	3.089(10)	Na1B-O4_$4	2.57(1)	Na9A-O37	2.86(5)	Na19-O44	2.63(2)	<S13-O>	1.509
<Ca8-O>	2.834	Na1B-O1	2.58(2)	Na9A-O32_$2	2.86(4)	Na19-O45_$1	2.661(13)	S14-O14A	1.509(5)
Ca9-O13A	2.140(12)	Na1B-O5	2.66(2)	Na9A-O38_$6	2.96(4)	Na19-O48_$1	2.70(2)	S14-O14B	1.515(5)
Ca9-O55_$1	2.48(2)	Na1B-O2_$3	2.69(1)	<Na9A-O>	2.800	<Na19-O>	2.580	<S14-O>	1.511
Ca9-O55	2.48(2)	Na1B-O6	2.71(2)						

Notes: Symmetry operators $1: –y+1, x–y, z; $2: –x+y+1, –x+1, z; $3: x–y, x, –z; $4: –y, x–y, z; $5: –x+y, –x, z; $6: –y+1, x–y+1, z; $7: –x+y, –x+1, z; $8: y, –x+y, –z+1; $9: –x+1, –y+1, –z+1; $10: –x, –y, –z+1; $11: x–y, x, –z+1; $12: y, –x+y, –z; $13: x, y+1, z; $14: x, y–1, z; $15: –x, –y, –z.

sodalite cages (S), and 6 cancrinite cages (C) within the unit cell. Considering the near absence of CO_3 groups shown by FTIR, essentially only SO_4 anion groups are present in bystrite and sodalite cages that would account for a maximum of 33 (SO_4) groups; considering in addition that H_2O molecules are contained in the cancrinite-type cages, a maximum of 6 H_2O molecules are present in fantappièite. A peculiarity of the fantappièite structure is the unique sequence of cages, while two or three different sequences of cages are found in other complex sequences (Bonaccorsi and Merlino 2005). In fantappièite, adjacent sequences are shifted by 1/3 along [001], ordered as SSBSSCCSSBSS (Fig. 4).

As described above, fantappièite is the first mineral belonging to the cancrinite group having an odd number of layers; although this would imply a rhombohedral lattice with space group $R\bar{3}m$, the real symmetry is $P\bar{3}$ due to ordering of extra-framework cations and anions. From inspection of Table 4, the mean T-O bond distances do not suggest a clear ordered pattern, which would justify the absence of mirror planes. However, based on the small size of the studied crystal, the presence of multiple twinning and the large number of atoms in the model, the possibility of Si,Al ordering in such a complicated structure cannot be ruled out.

Site assignment

While the observed bond lengths do not support (Si,Al) ordering in the framework tetrahedral sites, the composition (Table 1) is compatible with an Si:Al ratio of 1:1, which in most feldspathoids structures is usually related to order, following Löwenstein's rule (Löwenstein 1954). The site assignment for extra-framework cation sites (Table 8) in such a complicated structure is not easily determined. The overall number of electrons per formula unit (1750.3 epfu) and total cation sum ($Ca_{30.2}K_{14.8}Na_{78.7}$) agrees reasonably well (within a 0.5%) with the composition observed by EMPA and reported in Table 1, corresponding to ($Ca_{30.0}K_{16.0}Na_{84.1}$) and 1829.1 epfu.

The anion groups within the cages have a refined site occupancy for S of 23.6 apfu, lower than the content obtained by EMP analyses (30.24 apfu, see Table 1). Also the refined occupancy for Cl is higher than analyzed (2 apfu vs. 0.84 apfu in Table 1), although the agreement is better using (Cl+F) from EMPA. The reason for the 22% difference between the analyzed S content and the observed site occupancy can be explained based on the difficulties in locating the (SO_4) groups in the sodalite cages, which are probably highly disordered; for most of these groups, it was not possible to find feasible positions for O atoms in the Fourier difference map. By contrast, both site occupancy and coordinated O atoms of the (SO_4) groups in bystrite cages are reasonably refined with a soft constraint.

Relation to other species

Fantappièite is the member of the cancrinite group with the highest number of layers in the stacking sequence (33) discovered so far. Careful inspection of the sequence (Fig. 4) reveals that the structure of fantappièite can be derived from that of sodalite by inserting a shifted layer every 10 layers (shadowed layer in

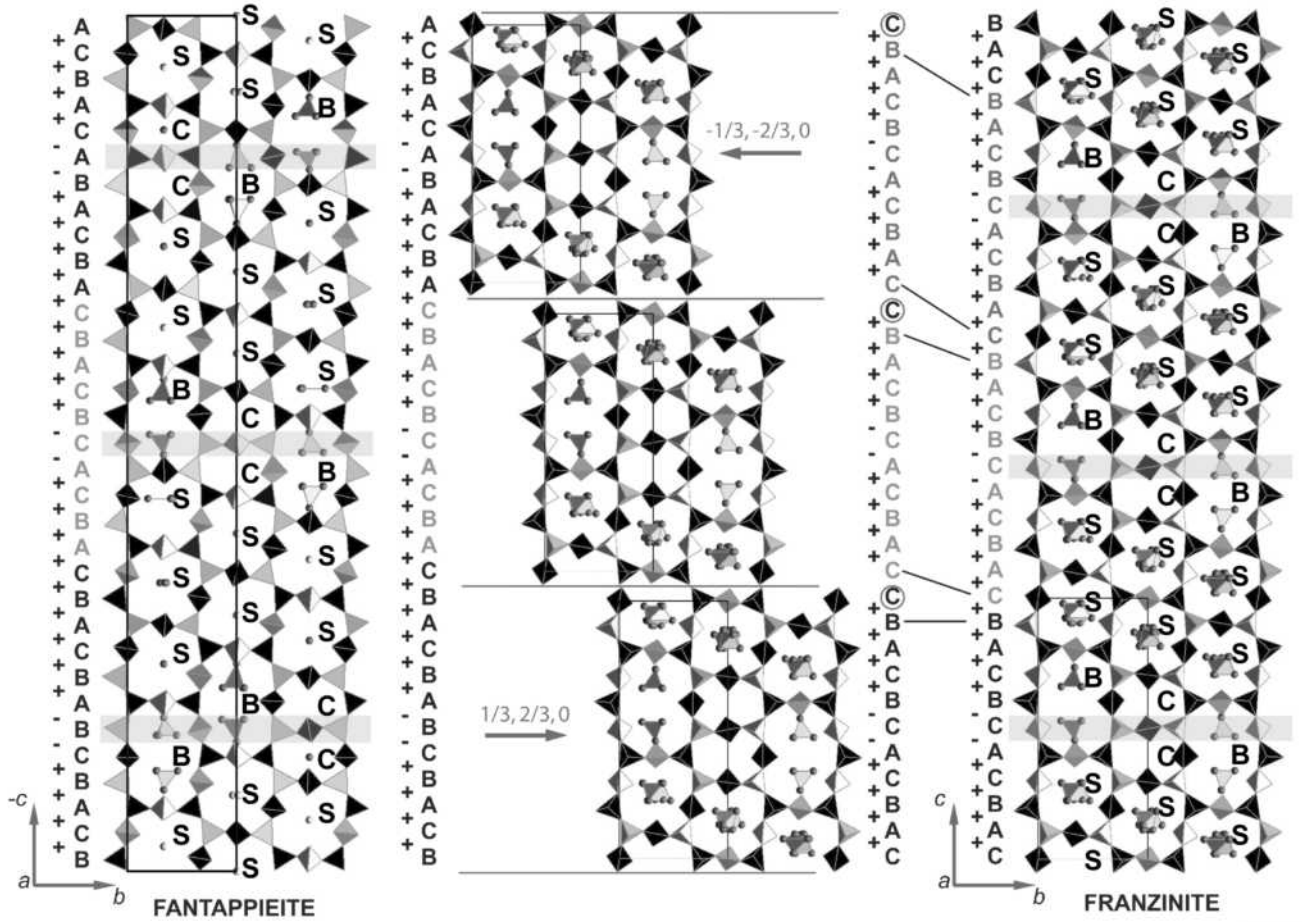

Figure 4. Comparison of the structures of fantappièite and franzinite (from Ballirano et al. 2000). Letters and signs of the sequences are shown. The projection in the middle shows their relationship. Inserted layers (with respect to franzinite structure) have the letter circled. In both fantappièite and franzinite, the layers inserted on the sodalite sequence are shown shadowed. The stacking sequence of cages along [001] is also shown for both structures. C = cancrinite cage; S = sodalite cages; B = bystrite cage.

TABLE 8. Site assignment for alkali sites in fantappièite

Atom	s.s. (epfu)*		*m*	s.o.f.†		Site population	
	split‡	Σ		spilt	Σ	(epfu)	(apfu)
Ca1		20.0	3		1.00	40.0	2.00 Ca
Ca2		16.9(3)	1		0.85	101.6	3.96 Ca + 2.04 Na
Ca3		20.0	3		1.00	40.0	2.00 Ca
Ca4		14.4(2)	1		0.72	86.5	2.28 Ca + 3.72 Na
Ca5		20.0	3		1.00	40.0	2.00 Ca
Ca6		12.4(3)	1		0.62	74.6	0.96 Ca + 5.04 Na
Ca7		20.0	3		1.00	40.0	2.00 Ca
Ca8		18.7(5)	3		0.94	37.4	1.87 Ca + 0.13 □
Ca9		20.0	3		1.00	40.0	2.00 Ca
Ca10		11.4(2)	1		0.57	68.7	0.30 Ca + 5.70 Na
Ca11		20.0	3		1.00	40.0	2.00 Ca
K1		15.0(3)	1		0.79	90.0	3.00 K + 3.00 Na
K2		15.3(2)	1		0.80	91.9	3.24 K + 2.76 Na
K3		18.8(2)	1		0.99	113.0	5.88 K + 0.12 Na
Na1A	6.0(1)		1	0.54		33.0	3.00 Na
Na1B	7.6(3)	13.6	1	0.69	1.23	45.4	1.62 Na + 1.38 Ca
Na2		4.5(3)	3		0.41	9.0	0.82 Na + 1.18 □
Na3A	10.1(3)		3	0.92		20.2	1.38 Na + 0.25 Ca
Na3B	3.7(3)	13.9	3	0.34	1.26	7.4	0.37 Ca
Na4A	5.8(1)		1	0.53		34.8	3.16 Na
Na4B	3.7(2)	9.5	1	0.33	0.86	22.2	2.02 Na + 0.82 □
Na5A	5.5(1)		1	0.50		33.0	3.00 Na
Na5B	10.4(3)	15.9	1	0.92	1.45	60.0	3.00 Ca
Na6		4.1(3)	3		0.37	8.3	0.75 Na + 0.25 □
Na7		4.3(3)	3		0.39	8.6	0.78 Na + 0.22 □
Na8		9.5(5)	3		0.86	18.9	1.72 Na + 0.28 □
Na9A	1.7(1)		1	0.15		10.2	0.93 Na + 0.76 □
Na9B	7.9(2)	9.5	1	0.72	0.87	47.4	4.31 Na
Na10	6.7(2)		3	0.61		10.7	0.90 Na + 0.04 Ca
Na11	10.7(4)	17.4	3	0.97	1.59	21.2	1.06 Ca
Na12	4.5(1)		1	0.41		27.0	2.45 Na
Na13	3.7(2)	8.3	1	0.34	0.75	22.2	2.02 Na + 1.53 □
Na14	5.4(2)		3	0.49		10.8	0.98 Na + 0.02 □
Na15	9.8(4)	15.2	3	0.89	1.38	19.6	0.98 Ca + 0.02 □
Na16	9.1(1)		1	0.82		109.2	2.40 K + 0.60 Na
Na17	5.3(2)	14.4	1	0.48	1.31	33.0	3.00 Na
Na18		12.1(4)	3		1.10	24.2	1.73 Na + 0.27 K
Na19		9.0(2)	1		0.82	53.9	4.90 Na + 1.10 □
Na20		7.1(4)	3		0.65	14.2	1.29 Na + 0.71 □
Na21		10.0(3)	1		0.91	60.0	5.45 Na + 0.55 □
Na22	9.2(1)		1	0.83		55.3	1.86 Na + 1.74 Ca
Na23	4.4(2)	13.6	1	0.40	1.24	26.4	2.40 Na
Na24		9.0(5)	3		0.82	18.0	1.64 Na + 0.36 □
Na25		10.4(3)	2		0.94	31.2	2.84 Na + 0.16 □
Na26		8.3(6)	6		0.75	8.3	0.75 Na + 0.25 □
sum		462.4			32.2	1750.3	30.19 Ca + 14.79 K + 78.68 Na

Note: *m* = site multiplicity; □ = vacancy.
* s.s. = observed site scattering.
† Refined with the atom species naming the site.
‡ split = the s.s./(s.o.f.) of pairs of split sites that are reported individually iwth corresponding errors; Σ = sum of s.s./(s.o.f.) at split sites and observed values at non-split sites.

Fig. 4). Alternatively, it can be considered as an ordered mixed sequence of interstratified franzinite plus a single layer (marked with a circle in Fig. 4), with a shift of (1/3, 2/3, 0) every 11 layers along [001]. Figure 4 displays the relationship between the franzinite and fantappièite structures. The structure of franzinite can be derived from that of sodalite by inserting a shifted layer every 9 layers (see Fig. 4; the shifted layer has been also shadowed). In this regard, it is worth noting that the FTIR spectrum of fantappièite is very similar to that of franzinite (Fig. 2).

Compared with the previous description of the unknown mineral done by Ballirano (1994), fantappièite has the same lattice cell parameters, and a very similar composition, FTIR spectrum, and X-ray diffraction powder pattern. However, the sequence proposed by Ballirano (1994), although consisting of the same number of layers, is different (ABCABCABCAB-BCABCABCABCCABCABCABCA) as no consecutive repetition of letters is found in the fantappièite sequence. The fantappièite sequence is fully compatible with a rhombohedral cell, as it can be expressed as composed of 3 blocks of 11 layers shifted by one period with respect to the precedent. Interestingly, HRTEM images obtained by Ballirano (1994) were in fact in accordance with 3 blocks of 11 layers. Therefore, it is highly probable that the material studied by Ballirano (1994) was indeed fantappièite.

ACKNOWLEDGMENTS

Thanks are due to F.S. Stoppani for providing us with the sample, to Gian Carlo Parodi (Paris) for assistance with the EMP analyses, Roberto Pucci for the microphotographs of fantappièite, and Roberto Gastoni (IGG-Pavia) for polishing and probe mounting. The suggestions of Yongjae Lee, T.M. Gesing, R. Peterson, and an anonymous reviewer, helped to improve the quality of the manuscript. Financial support to F.C. was provided by CNR-IGG, project TAP01.004.002, and to L.B. by PRIN 2007, project "Complexity in minerals: modulation, phase transition, structural disorder." Part of this work was done at the Laboratoire de Minéralogie, Museum National d'Histoire Naturelle, Paris, thanks to the support from the SYNTHESYS Project (http://www.synthesys.info/), financed by European Community Research Infrastructure Action under the FP6 "Structuring the European Research Area" Programme.

REFERENCES CITED

ASTM Standard E384 08ae1 (2008) Standard Test Method for Microindentation Hardness of Materials. ASTM International, West Conshohocken, Pennsylvania, DOI: 10.1520/E0384-08AE01, www.astm.org.

Ballirano, P. (1994) Crystal chemistry of cancrinites. Plinius, 11, 81–86.

Ballirano, P., Maras, A., and Buseck, P.R. (1996) Crystal chemistry and IR spectroscopy of Cl^- and SO_4^{2-} bearing cancrinite-like minerals. American Mineralogist, 81, 1003–1012.

Ballirano, P., Bonaccorsi, E., Maras, A., and Buseck, P.R. (1997) The crystal structure of afghanite, the eight-layer member of the cancrinite group: Evidence for long-range Si, Al ordering. European Journal of Mineralogy, 9, 21–30.

Ballirano, P., Bonaccorsi, E., Maras, A., and Merlino, S. (2000) The crystal structure of franzinite, the ten-layer mineral of the cancrinite-group. Canadian Mineralogist, 38, 657–668.

Bonaccorsi, E. and Merlino, S. (2005) Modular microporous minerals: Cancrinite-davyne group and CSH phases. In G. Ferraris and S. Merlino, Eds., Micro- and Mesoporous Mineral Phases, 57, p. 241–290. Reviews in Mineralogy and Geochemistry, Mineralogical Society of America and the Geochemical Society, Chantilly, Virginia.

Bonaccorsi, E. and Orlandi, P. (2003) Marinellite, a new felspatoid of the cancrinite-sodalite group. European Journal of Mineralogy, 15, 1019–1027.

Burla, M.C., Caliandro, R., Camalli, M., Carrozzini, B., Cascarano, G.L., De Caro, L., Giacovazzo, C., Polidoria, G., and Spagna, R. (2005) SIR2004: An improved tool for crystal structure determination and refinement. Journal of Applied Crystallography, 38, 381–388.

Chukanov, N.V., Rastsvetaeva, R.K., Pekov, I.V., and Zadov, A.E. (2007) Alloriite, $Na_5K_{1.5}Ca(Si_6Al_6O_{24})(SO_4)(OH)_{0.5}H_2O$, a new mineral species of the cancrinite group. Geology of Ore Deposits, 49, 752–757.

Chukanov, N.V., Rastsvetaeva, R.K., Pekov, I.V., Zadov, A.E., Allori, R., Subkova, N.V., Giester, G., Pushcharovsky, D.Yu., and Van, K.V. (2008) Biachellaite $(Na,Ca,K)_8(Si_6Al_6O_{24})(SO_4)_2(OH)_{0.5}.H_2O$, a new mineral of the cancrinite group. Proceedings of the Russian Mineralogical Society, 137, 57–66 (Russian with English abstract).

Della Ventura, G., Bellatreccia, F., and Bonaccorsi, E. (2005) CO_2 in minerals of the cancrinite-sodalite group: pitiglianoite. European Journal of Mineralogy, 17, 847–851.

Della Ventura, G., Bellatreccia, F., and Piccinini, M. (2008) Channel CO_2 in feldspathoids: New data and new perspectives. Rendiconti Lincei, 19, 141–159.

De Rita, D. and Zanetti, G. (1986) Caratteri vulcanologici e deposizionali delle piroclastiti di Stracciacappe (Sabatini Orientali, Roma). Memorie della Società Geologica Italiana, 35, 667–677.

De Rita, D., Funiciello, R., Corda, L., Sposato, A., and Rossi, U. (1993) Volcanic Units. In M. Di Filippo, Ed., Sabatini Vulcanic Complex. Progetto Finalizzato di Geodinamica, Quaderni de La Ricerca Scientifica, Monografie finali, 11, 33–79.

Downs, R.T., Bartelmehs, K.L., Gibbs, G.V., and Boisen Jr., M.B. (1993) Interactive software for calculating and displaying X-ray or neutron powder diffractometer patterns of crystalline materials. American Mineralogist, 78, 1104–1107.

Gunter, M.E., Downs, R.T., Bartelmehs, K.L., Evans, S.H., Pommier, C.J.S., Grow, J.S., Sanchez, M.S., and Bloss, F.D. (2005) Optic properties of centimeter-sized crystals determined in air with the spindle stage using EXCALIBRW. American Mineralogist, 90, 1648–1654.

Holland, T.J.B. and Redfern, S.A.T. (1997) Unit cell refinement from powder diffraction data: the use of regression diagnostics. Mineralogical Magazine, 61, 65–77.

Ihinger, P.D., Hervig, R.L., and McMillan, P.F. (1994) Analytical methods for volatiles in glasses. In M.R. Carroll and J.R. Holloway, Eds., Volatiles in Magmas, 30, p. 67–121. Reviews in Mineralogy, Mineralogical Society of America, Chantilly, Virginia.

Löwenstein, W. (1954) The distribution of aluminum in the tetrahedra of silicates and aluminates. American Mineralogist, 39, 92–96.

Mandarino, J.A. (1981) The Gladstone-Dale relationship: Part IV. The compatibility concept and its application. Canadian Mineralogist, 19, 441–450.

Moenke, H.H.W. (1974) Silica, the three-dimensional silicates, borosilicates and beryllium silicates. In V.C. Farmer, Ed., The Infrared Spectra of Minerals, p. 365–382. The Mineralogical Society, London.

Oxford Diffraction (2006) CrysAlis CCD (Version 1.171.31.2), CrysAlis RED (Version 1.171.31.2), and ABSPACK in CrysAlis RED. Oxford Diffraction, Abingdon, Oxfordshire.

Patterson, A.L. and Kasper, J.S. (1959) Close packing. In J.S. Kasper and K. Lonsdale, Eds., International Tables for X-ray Crystallography, Vol II, p. 342–354. The Kynoch Press, Birmingham.

Pouchou, J.L. and Pichoir, F. (1985) "PAP" $\Phi(\rho Z)$ procedure for improved quantitative micro-analysis. In J.T. Armstrong, Ed., Microbeam Analysis, p. 104–106. San Francisco Press, California.

Rastsvetaeva, R.K. and Chukanov, N.V. (2008) Model of the crystal structure of biachellaite as a new 30-layer member of the cancrinite group. Crystallography Reports, 53, 981–988.

Rastsvetaeva, R.K., Ivanova, A.G., Chukanov, N.V., and Verin, I.A. (2007) Crystal structure of alloriite. Doklady Earth Sciences, 415, 815–819.

Rinaldi, R. and Wenk, H.R. (1979) Stacking variations in cancrinite minerals. Acta Crystallographica, A35, 825–828.

Ross, S.D. (1974) Sulphates and other oxy-anions of Group VI. In V.C. Farmer, Ed., The Infrared Spectra of Minerals, p. 423–444. The Mineralogical Society, London.

Rozenberg, K.A., Sapozhnikov, A.N., Rastsvetaeva, R.K., Bolotina, N.B., and Kashaev, A.A. (2004) Crystal structure of a new representative of the cancrinite group with a 12-layer stacking sequence of tetrahedral rings. Crystallography Reports, 49, 635–642.

Sheldrick, G.M. (2008) A short history of SHELX. Acta Crystallographica, A64, 112–122.

Spek, A.L. (2008) PLATON, A Multipurpose Crystallographic Tool. Utrecht University, The Netherlands.

Su, S.C., Bloss, F.D., and Gunter, M.E. (1987) Procedures and computer programs to refine the double variation method. American Mineralogist, 72, 1011–1013.

Wilson, A.J., Ed. (1992) International Tables for X-ray Crystallography, vol. C. Kluwer Academic Publishers, Dordrecht.

Zhdanov, G.S. (1945) The numerical symbol of close packing of spheres and its application in the theory of close packings. Comptes rendus de l'Académie des Sciences de l'Union des Républiques Soviétiques Socialistes, 48, 39–42.

Manuscript received April 29, 2009
Manuscript accepted October 28, 2009
Manuscript handled by Lars Ehm